

Surface Residual Stress Tailoring of 420 Martensitic Stainless Steel by Laser Shock Peening

Aprilia Aprilia¹, Niroj Maharjan², Jin Lee Tan¹ and Wei Zhou^{1,#}

¹ School of Mechanical and Aerospace Engineering, Nanyang Technological University, 50 Nanyang Avenue, Singapore, 639798, Singapore

² Advanced Remanufacturing and Technology Centre, 3 CleanTech Loop, Singapore, 637143, Singapore

Corresponding Author / Email: mwzhou@ntu.edu.sg or wzhou@cantab.net, TEL: +65-6790-4700, FAX: +65-6792-4062

KEYWORDS: Laser shock peening, Martensitic stainless steel, Residual stress, Thermal effect, Microhardness

Laser shock peening is a surface enhancement method that is capable of altering the mechanical properties of materials. High energy pulsed laser beam is used to create shock waves that propagate through the material to induce compressive residual stresses. These compressive stresses are often beneficial for engineering components as they increase the crack resistance of the material. In this study, the laser shock peening of an annealed AISI 420 martensitic stainless steel (AISI 420SS) was studied. It was discovered that the microhardness and surface residual stress of a laser shock peened AISI 420SS sample varied significantly with the existence of ablative coating during the peening process. This finding shows that there is a potential to use ablative coating modifications in a laser shock peening process, to specifically tailor the surface residual stress of an AISI 420 martensitic stainless steel.

1. Introduction

Surface residual stress is the stress that remains near the top surface of a material when no external force or thermal gradient is applied. This stress is important for engineering components as it largely influences the lifespan of the part [1]. Most failures in engineering parts are originated on the surfaces in the form of fatigue failures [2]. Cyclic loadings of forces introduce cracks and propagate them over time. High surface compressive residual stress can help in hindering the formation and propagation of these cracks [3], thus extending the service life of the part.

AISI 420 martensitic stainless steel (AISI 420SS) is a high chromium stainless steel that has been widely used in valve, aerospace, and pump industries due to its high plasticity, shock resistance, and corrosion resistance properties [4, 5]. However, its applications in some industries are still limited due to the low hardness and poor wear resistance properties of the material [6-8]. Laser shock peening could be a useful surface modification method for AISI 420 martensitic stainless steel as it is capable of altering the mechanical properties of the material, such as residual stress and hardness. High energy pulsed laser beam is used to create shock waves in the material inducing compressive residual stresses and higher hardness.

This study investigated the surface residual stress tailoring of AISI 420 martensitic stainless steel by laser shock peening. Past studies on this topic are reviewed and only few papers studied laser shock peening of AISI 420SS. Wang et al. [9-11] investigated the laser shock peening of hardened and tempered AISI 420SS.

Nanosecond pulsed laser with laser spot diameter of 3 mm at different pulse energies of 3.6 J, 5.6 J and 7.6 J were used. Surface residual stress distribution, corrosion resistance, erosion resistance and structure changes were investigated. Maharjan et al [12] used a femtosecond pulse laser instead of a nanosecond pulse laser to do the laser shock peening of an annealed AISI 420SS. They found that femtosecond laser can also induce peening effect but at a much smaller depth (around 20-30 μm). They concluded that the state of residual stresses mainly depends on four factors: intensity of ablation-induced shock wave, thermal effect of laser beam, phase transformation of steel and surface mechanisms.

In this study, nanosecond pulse laser shock peening of an annealed AISI 420SS was explored. Microstructure, microhardness and surface residual stress changes were investigated. Surface residual stress variations of regions with and without laser and material direct interactions were also investigated.

2. Material and experimental procedures

2.1 Materials

AISI 420 martensitic stainless steel with the chemical composition shown in Table 1 was used in this study. The specimen size was 40 mm x 40 mm x 10 mm. The as-received specimen was subjected to a standard stress relief heat treatment by heating in an air furnace at 650 °C for 2 hours. It was then ground with SiC papers up to 1200 grit size prior to the laser shock peening.

Table 1 Chemical composition (wt.%) of the as-received AISI 420 martensitic stainless steel.

C	Si	Mn	Cr	Ni	Cu	Mo	V	Fe
0.41	0.33	0.74	12.69	0.16	0.05	0.05	0.046	Bal.

2.2 Laser shock peening

Laser shock peening was carried out using a high energy Q-switched Nd:YAG laser system (YS120-R200A) with the wavelength of 1064 nm and at repetition rate of 4 Hz, from Xi'an Tyrida Optical Electric Technology Co., Ltd. Nanosecond pulse (18-ns pulse duration) laser with the diameter of 3 mm, pulse energy of 10 J and peak power density of 7.86 GW/cm² was utilized. Peening with 50% overlap and 316% coverage was carried out. Coverage means the average number of times a point on the surface is peened, whereas the overlap defines the overlapping area percentage of adjacent laser spots [13]. Fig. 1 shows the photo of the shock-peened sample. Despite the use of ablative coating (polyvinyl chloride tape), some burnt marks appear on the peened surface. This generally occurs when the coating is removed during the peening process, exposing metal surface to direct contact with laser beam, hence the marks. The possible cause for ablative coating removal during the peening process could be due to improper application of the tape or rough surfaces. Air bubbles get trapped between the ablative coating and metal surface resulting in tearing of the coating, due to impact from laser beam. This tearing exposes nearby surface to direct laser beam. High laser power density could also be the cause of tearing.



Fig. 1 Photo of the laser shock peened sample showing regions without burnt-off coating (LSP) and with burnt-off coating (LSPboC).

2.3 Surface morphology and microstructure characterization

Top surface morphology was characterized using a 3D laser scanning confocal microscope, Keyence VK-X260K. The cross-sections were then mechanically ground and polished using standard metallographic sample preparation techniques. Samples were then etched with Kalling's No. 2 reagent (5 g CuCl₂, 100 ml HCl and 100 ml ethanol) for 10 seconds. Optical micrographs were obtained using light optical microscope Zeiss Axioskop 2 MAT. Secondary electron micrographs were obtained using scanning electron microscope JOEL 5600LV with accelerating voltage of 15 kV. Electron backscattered diffraction (EBSD) maps were obtained using JSM-7600F field emission scanning electron microscope with an accelerating voltage of 20kV and step size of 1 μm.

2.4 Microhardness and residual stress measurements

Microhardness indentation was carried out using the Vickers microhardness indenter Future-Tech FM-300e using load of 100 gf

and dwell time of 15 seconds. To obtain the average microhardness, five indentations were sampled at each location of interest. For the residual stress measurement, μ-X360 portable X-ray residual stress analyzer, based on cos α method was employed. Mn Kα radiation was used for the x-ray source and (311) diffraction peak at 2θ angle of 152° was used for the data collection and analysis.

3. Results and discussion

3.1 As-received AISI 420 martensitic stainless-steel characterization

Optical micrograph of the as-received specimen is shown in Fig. 2. An annealed microstructure with numerous randomly distributed spherical chromium carbides in the ferrite matrix is observed. The chemical composition analyses of these carbides and ferrite matrix are shown in Fig. 3.

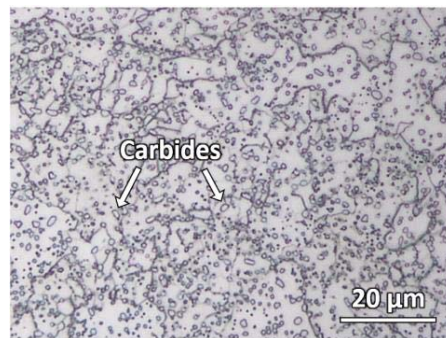


Fig. 2 Optical micrograph of the as-received AISI 420 SS.

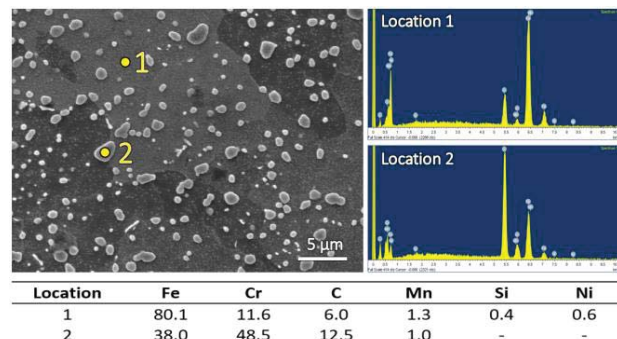


Fig. 3 Scanning electron micrograph (SEM) and energy dispersive spectroscopy (EDS) analysis of the as-received material showing the chemical compositions (wt.%) of the matrix and carbides.

EBSD grain boundary map and inverse pole figure (IPF-Y) map of the as-received material are shown in Fig. 4. The average grain size of the as-received material is 6.4 μm.

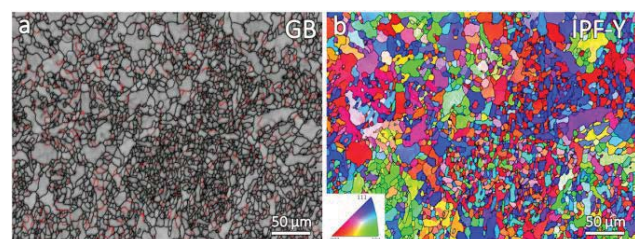


Fig. 4 (a) EBSD grain boundary map and (b) EBSD inverse pole figure (IPF-Y) map.

3.2 Top surface morphology of shock-peened sample.

Fig. 5 and Fig. 6 show the top surface morphology results of the LSP and LSPboC regions of the shock-peened sample. Surface roughness was calculated from three measurement data at three randomized locations. Results show that the surface roughness of the burnt-off region (LSPboC) is rougher (1.195 μm) than the region without burnt-off (0.898 μm). This is due to the surface ablation from the laser and material interaction.

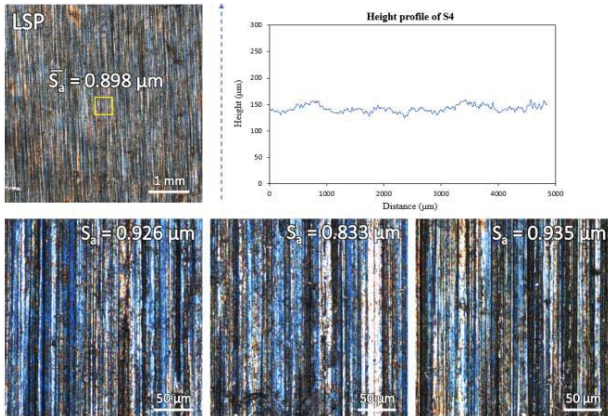


Fig. 5 Top surface morphology and surface roughness of the LSP region of shock-peened sample.

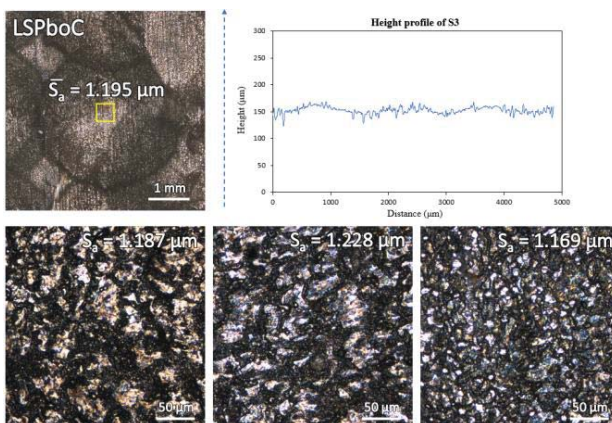


Fig. 6 Top surface morphology and surface roughness of the LSPboC region of shock-peened sample.

3.3 Microstructure characterization of shock-peened sample.

Fig. 7 presents the cross-section optical micrographs of the shock-peened sample after etching. Wavy-like surface due to the laser ablation can be observed in the peened surface area of the LSPboC region. Apart from that, both regions show similar microstructure with the as-received material. Undissolved carbides in the microstructure indicate minimal laser and material interaction.

Fig. 8 shows the EBSD maps of the shock-peened sample. From the grain boundary (GB) and kernel average misorientation (KAM) maps, it can be observed that there is a higher concentration of low angle grain boundaries and misorientations at the LSP region of the shock-peened sample than the LSPboC region. This shows that more deformations occurred at the LSP region than the LSPboC region. For the grain sizes, there is no observable differences between the two regions.

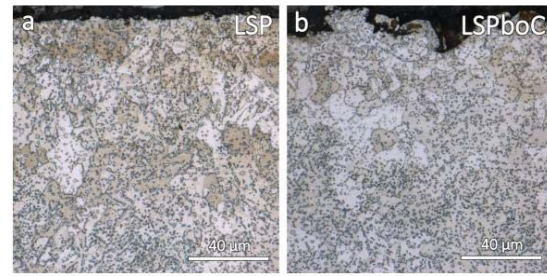


Fig. 7 Optical micrographs of the shock-peened sample: (a) LSP region (b) LSPboC region.

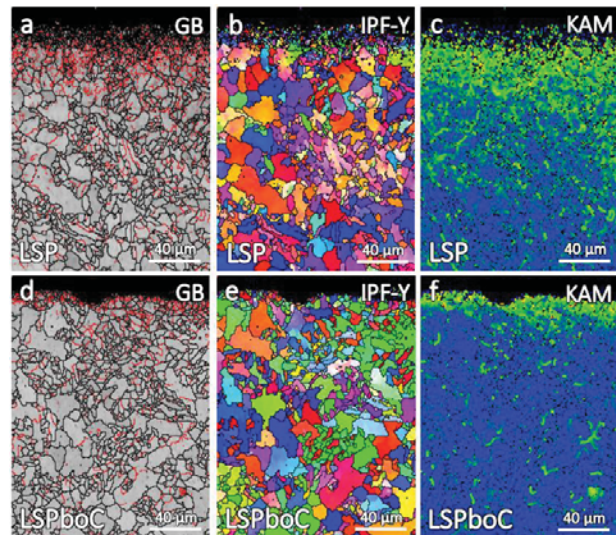


Fig. 8 EBSD maps of the shock-peened sample: (a-c) LSP region, (d-f) LSPboC region.

3.4 Microhardness characterization of shock-peened sample.

Fig. 9 shows the microhardness profile of the shock-peened sample. The as-received material has the microhardness of 173 ± 2 HV. After laser shock peening, the near top surface microhardness has increased to 218 HV for LSP region and 193 HV for LSPboC region. LSP region has a deeper hardened layer (about 3 mm) than the LSPboC region (about 1.5 mm). This shows that there is a higher shock wave effect at the LSP region when ablative coating is used. In the LSPboC region, the resulted shock wave effect is reduced and thermal effect is induced. Removal of coating does not only burn the surface but also reduce the depth of penetration. Ablative coating induces higher depth of effect possibly due to acoustic impedance mismatch effect.

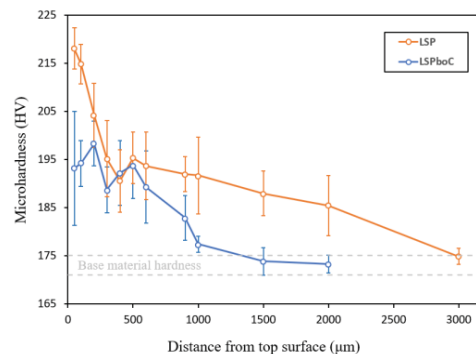


Fig. 9 Vickers microhardness profile of the shock-peened sample.

3.5 Residual stress measurement of shock-peened sample.

Surface residual stress results of the shock-peened sample are tabulated in Table 2.

Table 2 Surface residual stresses of the shock-peened sample.

Sample conditions	Residual stress	FWHM
LSP	- 619.4 MPa	2.76 deg
LSPboC	- 111.5 MPa	6.79 deg

As shown from the results, the induced compressive residual stress in LSP region is much higher than in the LSPboC region. This shows that the existence of ablative coating during the laser shock peening process is important. Without it, the shock wave effect is reduced, and the thermal effect is induced. These effects can change the resulted microhardness and residual stress of the material.

4. Conclusions

In this study, laser shock peening of an annealed AISI 420 martensitic stainless steel was studied. A nanosecond pulse laser with the laser beam diameter of 3 mm and pulse energy of 10 J was used. The results show that laser shock peening induces deformation to the annealed AISI 420SS at the form of high concentration of low angle grain boundaries and misorientations in the microstructure, high microhardness value, and high compressive residual stresses. The existence of ablative coating during the laser shock peening process was found to be critical. Without the coating, the shock wave effect is reduced tremendously, and thermal effect takes place. These result in different microhardness and surface residual stresses. This shows that the surface residual stress tailoring of AISI 420SS by laser shock peening can also be done by modifying the ablative coating. Further work is planned to test different ablative coating materials, thicknesses and designs using different laser pulse parameters.

ACKNOWLEDGEMENT

The authors would like to thank School of Mechanical and Aerospace Engineering, Nanyang Technological University for the research support.

REFERENCES

- Meyer, K., Denkena, B., Breidenstein, B. and Abrão, A. M., "Influence of residual stress depth distribution on lifecycle behaviour of AISI4140," *Procedia CIRP*, Vol. 87, pp. 450-455, 2020.
- Zhang, M., Pang, J., Meng, L., Li, S., Liu, Q., Jiang, A. and Zhang, Z., "Study on high-cycle fatigue fracture mechanism and strength prediction of RuT450," *Mater. Sci. Eng. A*, Vol. 821, pp. 141599, 2021.
- Pavan, M., Furfari, D., Ahmad, B., Gharghour, M. A. and Fitzpatrick, M. E., "Fatigue crack growth in a laser shock peened residual stress field," *Int. J. Fatigue*, Vol. 123, pp. 157-167, 2019.
- Yang, X. H., Jiang, C. M., Ho, J. R., Tung, P. C. and Lin, C. K., "Effects of Laser Spot Size on the Mechanical Properties of AISI 420 Stainless Steel Fabricated by Selective Laser Melting," *Materials*, Vol. 14, No. 16, pp. 4593, 2021.
- Dai, L. Y., Niu, G. Y. and Ma, M. Z., "Microstructure evolution and nanotribological properties of different heat-treated AISI 420 stainless steels after proton irradiation," *Materials*, Vol. 12, No. 11, pp. 1736, 2019.
- Mirshekari, G. R., Daei, S., Bonabi, S. F., Tavakoli, M. R., Shafyei, A. and Safaei, M., "Effect of interlayers on the microstructure and wear resistance of Stellite 6 coatings deposited on AISI 420 stainless steel by GTAW technique," *Surf. Interfaces*, Vol. 9, pp. 79-92, 2017.
- Shen, H., and Wang, L., "Mechanism and properties of plasma nitriding AISI 420 stainless steel at low temperature and anodic (ground) potential," *Surf. Coat. Technol.*, Vol. 403, pp. 126390, 2020.
- Sadhasivam, M., Sankaranarayanan, S. R. and Babu, S. K., "Synthesis and characterization of TiB₂ reinforced AISI 420 stainless steel composite through vacuum induction melting technique," *Mater. Today: Proc.*, Vol. 22, pp. 2550-2558, 2020.
- Wang, C., Luo, K., Bu, X., Su, Y., Cai, J., Zhang, Q. and Lu, J., "Laser shock peening-induced surface gradient stress distribution and extension mechanism in corrosion fatigue life of AISI 420 stainless steel," *Corros. Sci.*, Vol. 177, pp. 109027, 2020.
- Wang, C. Y., Cheng, W., Shao, Y. K., Luo, K. Y. and Lu, J. Z., "Cavitation erosion behaviour of AISI 420 stainless steel subjected to laser shock peening as a function of the coverage layer in distilled water and water-particle solutions," *Wear*, Vol. 470, pp. 203611, 2021.
- Wang, C., Luo, K., Wang, J. and Lu, J., "Carbide-facilitated nanocrystallization of martensitic laths and carbide deformation in AISI 420 stainless steel during laser shock peening," *Int. J. Plast.*, Vol. 150, pp. 103191, 2022.
- Maharjan, N., Lin, Z., Ardi, D. T., Ji, L. and Hong, M., "Laser peening of 420 martensitic stainless steel using ultrashort laser pulses," *Procedia CIRP*, Vol. 87, pp. 279-284, 2020.
- Maharjan, N., Chan, S. Y., Ramesh, T., Nai, P. G., Ardi, D. T., "Fatigue performance of laser shock peened Ti6Al4V and Al6061-T6 alloys," *Fatigue Fract. Eng. Mater. Struct.*, Vol. 44, No. 3, pp. 733-747, 2020.